J Porous Mater
DOI 10.1007/s10934-010-9406-0

Preparation and electrowetting transitions on superhydrophobic/hydrophilic bi-layer structures

Victor A. Lifton · Steve Simon

Abstract A simple method of preparing porous superhydrophobic materials using glass fiber materials, where hydrophobicity is provided by a variety of coatings such as self-assembled alkyl-silane monolayers and fluoropolymers such as Teflon is presented. Fibrous structures of the filter material provide for the modulation of "surface roughness" on the micro- and nano-scale, required for achieving a superhydrophobic state, with advancing contact angle of water on such surfaces close to 150 degrees. Such superhydrophobic structures are effective at separating water-octane mixtures by allowing only low-surface-tension component to go through the thickness of the material, while repelling the water (high-surface-tension component) and preventing it from permeating through the material. In addition, a bi-layer structure that combines a superhydrophobic surface with a highly hydrophilic bulk material is described. It is formed by subjecting superhydrophobic fiber material to a brief oxygen plasma treatment to remove the hydrophobic coating from one side of the material, whereas the opposite side is protected during treatment and remains superhydrophobic. Tunable properties of the superhydrophobic fiber material are demonstrated using electrowetting with PEDOT–PSS conductive polymer core, parylene as a dielectric and Teflon as a hydrophobic coating. Applicability of such bi-layer materials to microfluidic and energy storage micro-devices is discussed.

Keywords Electrowetting · Porous · Superhydrophobic · Filter · Battery · Conductive polymer

V. A. Lifton (✉) · S. Simon
mPhase Technologies, Inc., 150 Clove Rd, Little Falls, NJ 07424, USA
e-mail: vlifton@mphasetech.com

1 Introduction

Preparation of superhydrophobic surfaces and materials is an important and quite popular topic in surface science nowadays [1–3]. The phenomenon defined rather broadly can be visualized as a drop of liquid sitting on such surface forming a large contact angle, typically greater than 150 degrees for pure water, and easily rolling on or sliding off of such surface. McCarthy and co-authors have additionally suggested that both contact angle and contact angle hysteresis should be taken into account to call a surface "superhydrophobic" [4, 5]. Coincidentally, they indicated that properties that are now referred to as "superhydrophobic" have been well known and documented in the textile industry since the early 1940's. In their report [4] they demonstrated "an artificial lotus leaf prepared using a 1945 patent and a commercial textile." A variety of superhydrophobic materials have been prepared and reported in the literature, too numerous to mention here, with a few cited for reference [1–3, 6, 7]. A plethora of methods such as nanofabrication, electrospinning and wet etching have been employed to prepare these materials. As a rule of thumb, both micro and nano-scale roughness are created on the surface of the sample, which is subsequently treated with a thin hydrophobic coating rendering the surface superhydrophobic. Since thorough analysis of the phenomenon of superhydrophobicity is beyond the scope of this paper, we refer interested readers to the literature dealing with this topic in greater details [1–3, 8, 9]. A more general case of the superhydrophobic surfaces are the so called superlyophobic [10] or superoleophobic surfaces [11]. They are characterized by a high contact angle (>150 degrees) of not only inorganic high-surface-tension liquids such as water but also of organic low-surface-tension liquids such as oil and alcohols. They have also been referred

Published online: 29 August 2010

to as omniphobic surfaces or, in other words, as universally repelling surfaces [12].

Biological structures with surface properties very similar to those demonstrated by superhydrophobic surfaces are abundant in nature. For example, a pioneering article by Neinhuis and Barthlott [13] cited 200 plants as having hydrophobic structures, combing both surface roughness and "waxy" overlayers. A recent review by the authors summarized some of the biomimetic work in this field [14]. One of the most commonly cited examples is the lotus leaf, with its remarkable ability to repel water and stay clean [15, 16]. A combination of micro- and nano-scale topography, covered with a hydrophobic wax, is thought to be responsible for the superhydrophobic behavior. Some insects developed superhydrophobic structures to collect water from the humid air and to channel it directly into their mouth [17]. Carnivorous plants have slippery (potentially superhydrophobic) regions composed of an entangled web of fibers to prevent prey from escaping [18]. In this example, a protruding fiber end, a kink or a bend in the fiber, may represent "surface roughness" required for exhibiting the superhydrophobic behavior. These are just a few examples of the "competitive" structures from nature. The last example is closely related to the type of superhydrophobic surfaces that are described in this manuscript.

Earlier, we have reported on the fabrication of tunable superhydrophobic surfaces using silicon nanofabrication [6, 10, 19]. We demonstrated a porous surface that could be switched from repelling a liquid to complete permeation of the liquid throughout the sample thickness using electrowetting. Such electrically-controlled tunability is obviously very attractive in a variety of microfluidic devices, including lab-on-a-chip detection and fluid delivery systems, given its simple control via logic electronics. Researchers are only beginning to test the viability of superhydrophobic materials in real-life applications. Several promising areas have been suggested, such as filters for separating hydrocarbons from water, anti-fog coating and self-cleaning surfaces [20–22]. Our group is currently using these materials in the design of energy storage devices (reserve micro-batteries), where superhydrophobic materials are employed in order to separate liquid electrolyte from solid electrode materials [19, 23, 24]. When a reserve battery is in an inactive state, the electrolyte is kept away from the electrodes, thus, extending the battery shelf life, by preventing self-discharge and unwanted chemical reactions.

A significant barrier to a wider use of these materials stems from their complicated synthesis and preparation. For example, if the nanostructures are based on silicon substrate, such processing requires a costly clean room equipped with complex photolithographic equipment, to image nano-sized surface features, followed by the etch steps in highly specialized tools. Using silicon substrates, the size of the final work piece is limited by the size of the wafer-handling equipment in the clean room, which is typically between 4 and 8 inches in diameter. In a different approach, nano-sized particles are synthesized and spread as a top-coating over a surface of interest to create nano-roughness [25]. While conceptually simple, such processes require access to chemical reactors and chemical procedures that may not be uniform or reproducible on a large scale. Attempts are also being made to utilize CVD-type processing for large-scale production [26]. Consequently, most methods can only produce superhydrophobic surfaces of limited size. New approaches are required to enable large scale production and treatment of these promising materials using off-the-shelf starting materials.

A combination of both superhydrophobic and hydrophilic properties on a single substrate has not yet been easily achieved, even though such combinations of properties can be beneficial for use in devices that require fluid transport, spreading and filtration. For example, hydrophobic/hydrophilic bi-layer material can be used to transport (wick) liquids throughout the hydrophilic layer, while spreading can simply be halted at the hydrophobic interface, thus, avoiding complex valves and pump structures.

The purpose of this paper is to present a simple method of preparing surfaces that combine properties typical for a superhydrophobic material (liquid repellency and very high contact angle) and for a hydrophilic material (rapid liquid spreading and wicking). We will show how to produce such bi-layer materials using commonly available materials such as glass fiber filters. Our approach is different from other attempts at preparing superhydrophobic materials using electrospinning and nano-fibers [27–29] because we are using commercially and readily available materials. Hydrophobic coatings are then prepared using the dip coating method, a very common industrial processing technique used to paint cars or to treat plastic surfaces in a continuous roll-to-roll configuration.

2 Materials and processing

2.1 Filter material

The substrate we chose for this work was a commercially available glass fiber filter, manufactured by Millipore Corporation (type APFC, 47 mm in diameter). A large number of other types of glass fiber filters are available from this and other manufacturers, with various pore sizes and fiber diameters and samples easily found in most lab supply catalogs. A micrograph of this material is given in Fig. 1; it is an interwoven collection of glass fibers of various diameters, mostly in sub-micron range. It has high

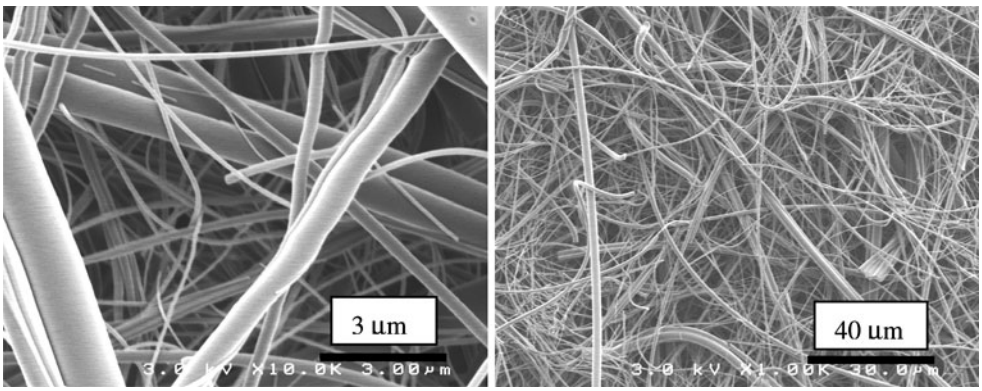

Fig. 1 SEM images of the as-received APFC glass fiber filter

porosity and a well developed surface area. The sub-micron size of its fibers creates surface "roughness" in the same range. Since it is made out of glass, it is chemically inert, thermally stable and at the same time flexible and compliant. This type of filter is highly hydrophilic and is capable of quickly absorbing large amounts of liquids. The filters tested were off the shelf items, used as received from the manufacturer.

2.2 Hydrophobic coatings

A variety of hydrophobic coatings are available and for the purposes of this work, we focused our attention on gathering results using inert coatings prepared from Teflon AF. The coatings were prepared via dip coating from 1% solution of Teflon AF 1600 in Fluorinert FC-84 perfluorinated liquid by 3 M. Dip coating was performed using a bench-top dip coater, TL0-01 (MTI Corp), at 0.1 mm/s pulling speed. The films were then dried in an oven at 200 °C for 2 h in nitrogen atmosphere.

In addition to preparing Teflon AF coatings as the main thrust of this work, we prepared other coatings using fluorinated polymer CYTOP CTL-809 M (Asahi Glass Co.), as well as self-assembled monolayers (SAM) of fluorinated and non-fluorinated alkyl silanes. All methods offer very convenient processing and can be tuned depending on the material and final device requirements. When low temperature processing is required, hydrophobic coatings based on self-assembled monolayers may be used to replace high temperature processing required for Teflon AF. Alternatively, drying at room temperature can be used with the hydrophobic coatings developed by Cytonix LLC (www.cytonix.com). We have successfully implemented these procedures on porous materials made from sintered stainless steel, woven wire mesh, PVDF, cellulose and nylon filter materials. Obviously, other materials and deposition methods are available but are beyond the scope of this paper.

2.3 Characterization

Contact angle measurements were performed using a VCA Optima XE system equipped with the droplet image analysis software (AST Products, Inc). In a typical test, a single droplet (volume 5 μl) was dispensed on the surface of the sample and the contact angle measurements were performed. At least three droplets for each test liquid were made. Test liquids have been chosen to cover a wide range of surface tension, from water (72 mN/m) to hexane (18.4 mN/m). All liquids were obtained from Alfa Aesar. To enhance contrast and improve image analysis, the liquids have been colored with a blue dye (Solvent Blue 38) or a red dye (Oil Red O).

The surface of the glass fiber material is not smooth, but covered with the dense "forest" of protruding fibers sticking above the surface (Fig. 1). This irregular geometry makes precise measurement of the contact angle somewhat difficult and results in larger than typical baseline (on flat surfaces) errors in the measurements ±5 degrees.

3 Results and discussion

After a hydrophobic coating was prepared on a filter material, contact angles were measured on the filter's surface using various liquids. Data for such tests on APFC filter treated with 1% Teflon coating are given in Table 1. For comparison, the contact angle on a flat SiO_2 surface treated in an identical manner is presented as well. There is a marked difference between the wetting properties of the surface of the flat sample and the surface of the filter sample. APFC surface is superhydrophobic, with the contact angle of DI water being 147 degrees [30]. As mentioned earlier, inherent non-uniformity of the filter's surface due to individual fibers and fiber bunches protruding above the surface and blurring the interface between the droplet and the filter surface made it difficult

Table 1 Contact angle on the flat SiO_2 and on APFC glass fiber filter surface treated with 1% Teflon solution

Liquid	Surface tension, mN/m	Planar substrate contact angle, degrees	Contact angle on Teflon treated APFC filter, degrees (advancing/receding)
Hexane	18.40	14.0	Spreads
Octane	21.60	28.7	Spreads
1-propanol	23.70	49.2	133/111
1-octanol	27.60	57.3	140/129
Cyclopentanol	32.70	66.5	142/132
Propylene carbonate	41.90	84.6	145/139
Water	72.75	119.0	147/138

to measure the precise values of the contact angle. We note that contact angle hysteresis was fairly large, about 10 degrees for all test liquids and can be attributed to a highly non-uniform surface of the filter due to protruding fibers that may pin the triple contact line. At the same time, it did not prevent the high-surface-tension liquids from exhibiting "rolling" ball behavior, where tilt induces rapid droplet sliding off the surface. Figure 2 shows droplets of the test liquids sitting on the superhydrophobic surface of APFC filter.

Of several organic liquids tested, low-surface-tension liquids such as n-hexane and n-octane (surface tension 18.4 and 21.6 mN/m, respectively) wetted the filter almost instantaneously. Even though other low-surface-tension organic liquids were supported by the filter's surface (in Cassie-Baxter state), we defer from calling this surface superlyophobic and prefer to stay with the term superhydrophobic. At the same time, such material can in fact be used to separate water/octane mixtures by effectively preventing water from going through the filter. The effect is similar to the results showed in [11] but differs in a substantially simplified processing of the superhydrophobic materials presented here.

Attempts to prepare plasma deposited fluorocarbon CFx type coatings on the surface of APFC filters have not been successful to date, perhaps because of the very high surface area of the filter that requires larger amounts of deposited coatings than are attainable in the deposition tool used in our work. APFC material coated with various SAM coatings (not presented here) showed trends in the contact angle data similar to the Teflon coated samples.

To show that the superhydrophobic properties exist throughout the thickness of the filter material and not only on its surface, the top layer was very carefully separated with a thin, flexible razor blade to expose fibers in the middle of the material. Contact angle measurements on this freshly formed surface revealed the contact angle of water of about 150 degrees, the same as measured on the top surface of the as-prepared material.

4 Bi-layer material preparation and characterization

We developed a very simple technique of preparing materials with bi-layer hydrophobic/hydrophilic properties. By bi-layer materials, we mean a material having a superhydrophobic surface on one side of the material and a highly hydrophilic surface on the other side. The easiest way to prepare such surfaces is to start with a glass fiber filter and deposit hydrophobic coating via self-assembly (for SAM) or dip coating (for Teflon), thus obtaining a superhydrophobic coating throughout the thickness of the material as described in the previous section. Then, by briefly exposing one side of the filter to O_2 plasma (for $\sim$30–240 s depending on the type of the coating), we remove the deposited coating from this side, which results in it becoming highly hydrophilic, as in the original pre-Teflon treatment state. At the same time, the opposite side still retains its superhydrophobic properties as evidenced by large contact angle. Thus, we produced a material with unique microfluidic properties, as it can quickly spread the liquid throughout its thickness, as well as laterally, until the superhydrophobic region within the material is reached and spreading is halted. A droplet of liquid placed on the superhydrophobic side forms a "rolling" ball state [6].

Figure 3 shows one such filter cut in half, along the diameter with the superhydrophobic side of one half, and O_2 plasma treated hydrophilic side of another half, both facing up. Five different liquids were placed on each sample and the results are clear, the superhydrophobic side supported all liquids in the Cassie-Baxter state without spreading or penetration inside the material, confirmed by the contact angle measurements presented in Fig. 2 and Table 1. Furthermore, the liquids can be shaken off without leaving stains on the surface. Contrary, the hydrophilic side easily absorbs the same liquids and wicks them across its surface. This is the same effect that was observed on the fresh, as-received untreated filter material. In Fig. 4, we flipped the superhydrophobic side upside down to show that no penetration into the filter material occurs, thus

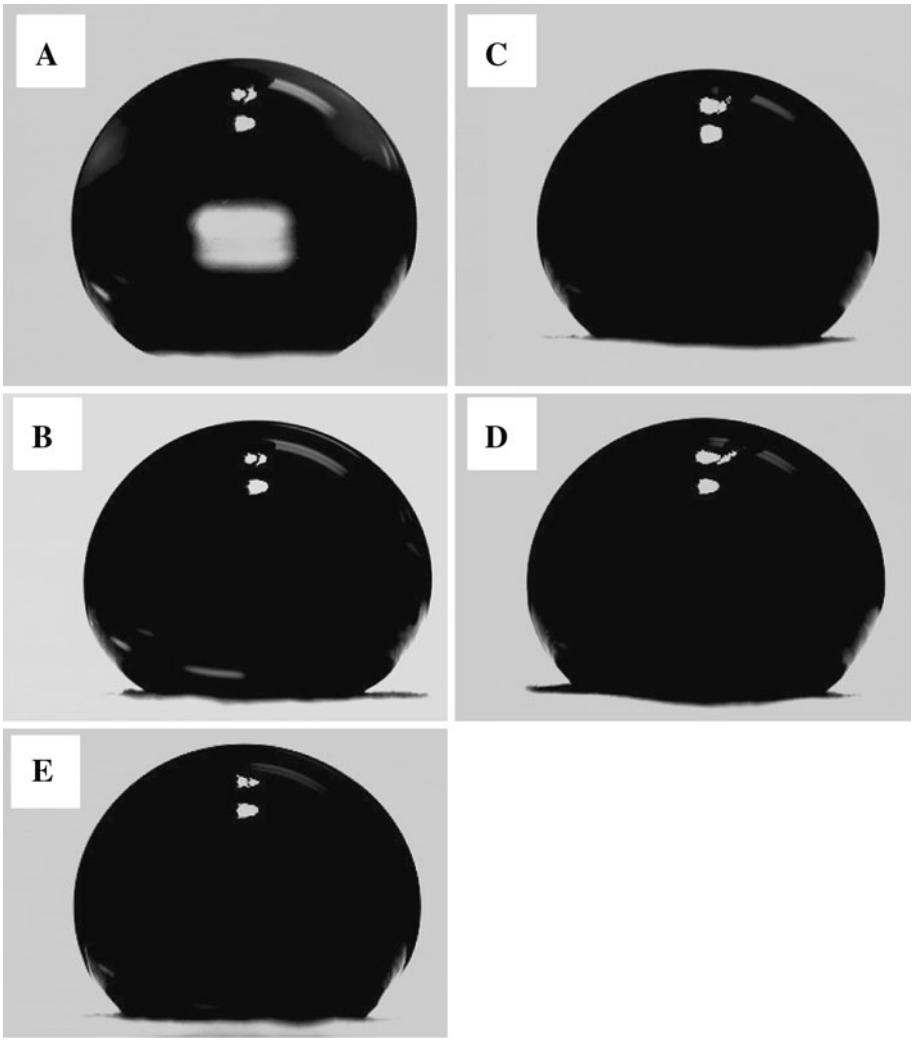

Fig. 2 Droplets of various test liquids sitting on the superhydrophobic surface of Teflon-treated APFC fiber filter. Images taken during contact angle measurement tests; surface tension is given for each liquid. **a** water (72 mN/m); **b** polypropylene carbonate (42 mN/m); **c** cyclopentanol (33 mN/m); **d** 1-octanol (28 mN/m); **e** 1-propanol (24 mN/m)

confirming that the liquids are sitting on the top of the surface roughness only, similar to other superhydrophobic surfaces. We are currently exploring the use of the bi-layer materials as separators in the electrochemical power cells [23, 24].

Our method provides ease of fabrication and control over the degree of hydrophobicity/hydrophilicity. One can envision masking off (protecting) certain regions on the superhydrophobic side, and performing O_2 plasma cleaning on the exposed area, to obtain alternating regions with various wetting behavior, similar to the work reported by Zimmermann and co-authors [31]. In addition, similar bi-layer properties can be achieved by layering hydrophobic/hydrophilic materials. One can also envision using bi-layer materials to construct low-cost lab-on-a-chip diagnostic devices similar to those described by Martinez and co-authors [32]. In that approach, the authors created microfluidic channels in paper impregnated with the cross-linked polymer, by cutting it with a laser cutter. The cross linked polymer helped repel and contain the liquid, whereas channels and wells were filled with cellulose powder to help wick the fluids between the adjacent layers. Using our approach, the task of creating complex microfluidic channels and wells will be simplified. The channels for transport by wicking would be etched in the otherwise superhydrophobic filter material. The remaining superhydrophobic material will encase the fluid moving inside of the channel and prevent it from spreading out.

A similar bi-layer approach has been used to create superhydrophobic/hydrophilic structures on anodic aluminum oxide (AAO) [33]. In this work, AAO has been synthesized in the shape of a thin porous membrane that was treated with plasma polymerized fluorocarbon polymer on one side only, creating a hydrophilic surface on the opposite side of the porous region. The authors of that work have not described if other porous materials can be used in place of AAO. In a related approach [34], a stack of cellulose paper has been treated in plasma in the presence of perfluoromethylcyclohexane, to produce hydrophobic material. However, it was noted that the hydrophobic

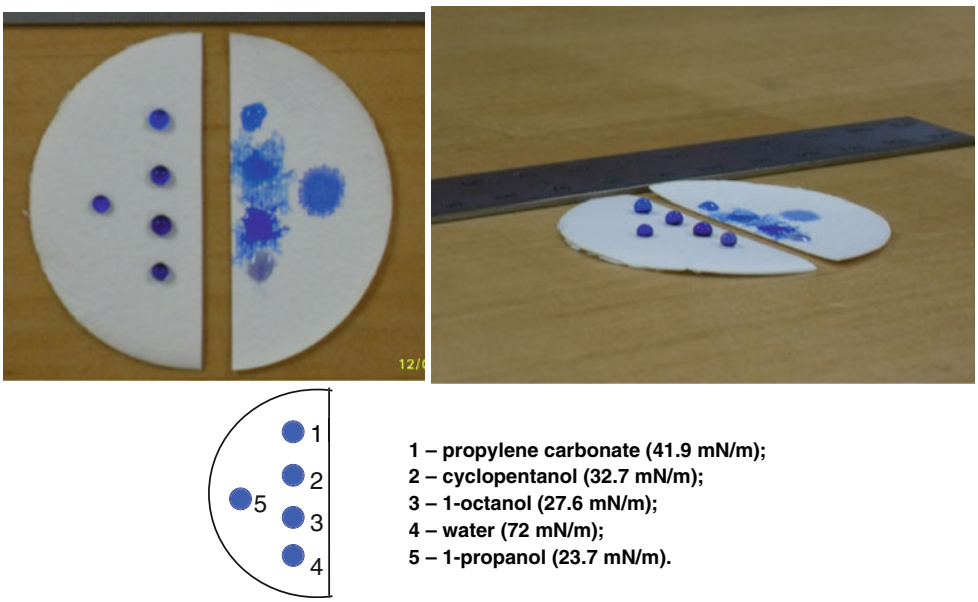

Fig. 3 Left hemi-circle of APFC filter has been treated with Teflon; right hemi-circle had its Teflon coating removed in oxygen plasma. Note the superhydrophobic behavior of the left side and regular wicking and liquid absorption on the right

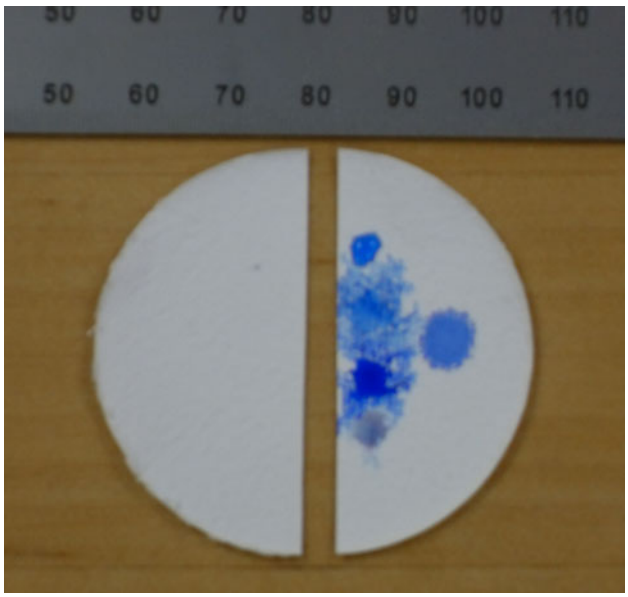

Fig. 4 The same left hemi-circle as in Fig. 3 but flipped over to show that no liquid penetration into the bulk of the filter material has occurred on the superhydrophobic side

treatment throughout the thickness of the stack is complicated and cannot be well controlled. In contrast, in our approach, the hydrophobic surface is created through the entire thickness of the material, which can later be modified if required.

Balu and co-authors [35, 36] presented a method of creating "roll-off" and "sticky" superhydrophobic cellulose materials using a 2-step plasma processing technique, combining selective plasma etching of amorphous regions in cellulose and fluorocarbon deposition. While such treatment results in a highly superhydrophobic state, the surface roughness modulation depends on the particular structure of cellulose that may not be available in other materials. The same group reported "lab-on-paper" devices using superhydrophobic paper patterned with less hydrophobic regions deposited with the ink, on a commercial Xerox Phaser printer [37].

We must emphasize that the glass fiber material is not the only material that can be prepared in this fashion to produce superhydrophobic materials. Similar filter materials can also be used. We have successfully prepared superhydrophobic materials using off the shelf cellulose, nylon, PVDF and metal mesh filters. Clearly, the choice is only limited by the temperature required to process hydrophobic coatings and chemical compatibility with the solvents.

5 Electrowettable glass fiber materials

5.1 Conductive fiber material preparation

Clearly, at this stage the bi-layer material is a "passive" material that does not have the ability to dynamically tune or change its wetting (or non-wetting) properties. As was indicated in the introduction, one method to change surface wettability is by employing a phenomenon called electrowetting. Controlled electrowetting transitions on the Si-based nanostructures have been described in [6, 10, 19]. Combining dynamic tunability with the bi-layer properties should give us even more flexibility in building microfluidic devices with multiple functions.

As a background, we recall that a typical structure for electrowetting (or, more proper for this case,

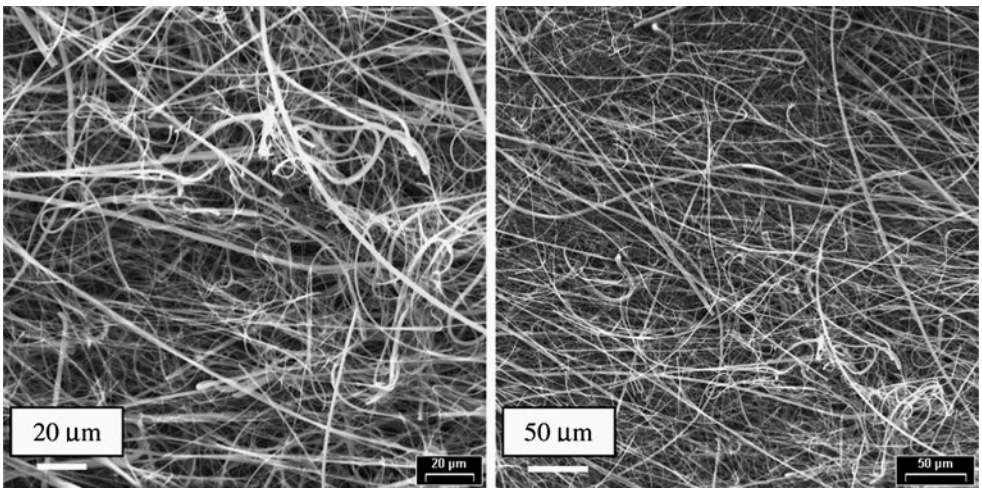

Fig. 5 SEM image of APFC fiber filter dip coated in the suspension of Baytron conductive polymer. The image is very similar to that of the untreated filter in Fig. 1

"electrowetting on dielectric") consists of a conductive core coated with a dielectric material and a hydrophobic coating. A significant difference between the structures prepared in this work and in the previously cited works, is the absence of the conductive core in the fiber materials presented here. Nanostructures from References [6, 10, 19] have been prepared from conductive silicon that was later oxidized to form a dielectric layer on the surface. Therefore, as the first step in making APFC material undergo an electrowetting transition, we would need to make the fiber material conductive. One way of doing this is to deposit a conductive layer covering the entire surface of all fibers in the material. This is a challenging problem given its complex 3D surface. Coating a corrugated surface using line-of-sight methods such as sputtering and evaporation to create a uniform conductive layer is extremely difficult and not consistently reproducible. Electroplating is not possible either, since the starting substrate is not conductive. Instead, we attempted to coat the fibers with conductive polymers deposited from aqueous solution via dip coating. Aqueous suspensions of conductive polymers are now commercially available and represent an intriguing alternative in creating conducive coating on a variety of substrates of complex shape. The vendor H.C. Stark now offers PEDOT/PSS–based conductive polymers as a commercial product under various names such as Baytron or, more recently, Clevious grades [38]. We obtained a sample of Baytron P, which is an aqueous dispersion of the intrinsically conductive polymer PEDOT/PSS [poly(3,4-ethylenedioxythiophene) poly(styrenesulfonate).

Dip coating was performed using the same conditions as previously described for Teflon dip coating. After pulling samples from the solution, they were let to air dry. It was observed that the filter material retained its flexibility and wicking ability after this treatment. Figure 5 shows an APFC filter covered with the uniform Baytron coating as evidenced by the absence of clumps or agglomerates. The fiber material looks essentially the same as in Fig. 1, except that conductive polymer coating makes it easier to image in the SEM by preventing charging.

In the next step, we covered this conductive layer with a layer of dielectric to form the capacitive structure for electrowetting tests. In our case, we decided to use vapor-deposited parylene. It has been widely used as a dielectric in various electronics devices and in multiple electrowetting tests we have conducted, and is an excellent choice because of its dielectric properties. Additionally, parylene is deposited from the vapor phase, assuring that it will uniformly coat the fiber surface. Once a layer of parylene was deposited, we once again performed dip coating, now in the solution of Teflon to form the hydrophobic layer. Both parylene and Baytron coatings have sufficient thermal stability to survive the post-deposition bake for Teflon coating at 200 °C. This approach is similar to the one used by Bhat and co-authors [39] to prepare electrowettable textiles. However, in our approach, we used a commercial fiber product instead of a custom made, laser drilled polymer. Agarwal and co-authors [40] used layer-by-layer self-assembly of poly(3,4-ethylenedioxythiophene)–poly (styrenesulfonate) (PEDOT–PSS) on lignocellulose wood microfibres to create "conductive paper".

Figure 6 compares structures prepared for electrowetting using Si substrate and APFC fiber material. Clearly, in both cases, Si nanoposts and glass fibers provide surface roughness and the frame for the dielectric and hydrophobic coating deposition.

Measurements of sheet resistance of the fiber material samples were complicated by the soft, compliant nature of

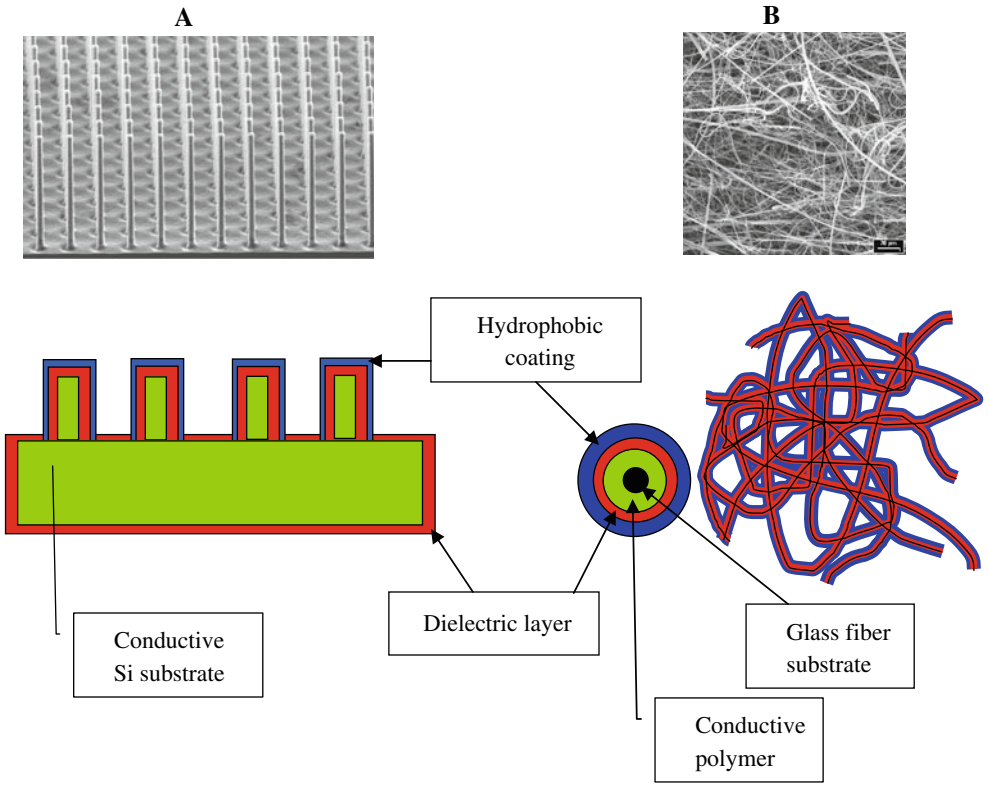

Fig. 6 Schematic cross-sections through **a** the Si nanostructured substrate (so called nanograss, see References 6, 23) and **b** APFC glass fiber materials showing essential elements of the microstructure required for the electrowetting transitions: hydrophobic coating, dielectric layer and conductive core. Actual SEM images of the corresponding structures are given as well

the glass fiber material that yields and deforms under a 4-point probe that is regularly used in this type of measurements. The estimate of sheet resistance is 30–100 kOhm per square. Such resistivity of Baytron P—impregnated APFC material is fairly high but we did not attempt to produce a truly "conductive" filter material. This, however, is not a requirement for the electrowetting transitions, since the process is based on capacitive charging and not on the dc current flow.

During short-term testing of the superhydrophobic properties of Baytron-impregnated APFC material using various liquids, we did not encounter any undesired chemical reactions or material degradation. In case the chemical stability ever becomes an issue and Baytron materials can no longer be used to create conductive layers, an alternative approach could be the use of carbon nanotube-filled ink, similar to the approach described in [41]. The authors impregnated commercial copy paper with a specially formulated carbon nanotube ink, achieving conductivity of 1 ohm per square. It was then integrated as a current collector in a supercapacitor and a Li-ion battery. Despite the aggressive nature of the electrolytes used in the construction of Li-ion batteries, the conductive paper performed well in these preliminary tests. The use of this type of ink is also attractive due to high thermal stability of carbon nanotubes. When used on highly chemically stable glass fiber materials as used in our work, more robust tunable bi-layer superhydrophobic/hydrophilic materials should be possible. Using conductive ink to create truly dc conductive fiber materials may be more attractive than using multiple impregnations with Baytron materials, as it tends to make the filter material more and more rigid with each cycle of impregnation.

5.2 Contact angle

Measured contact angle of DI water on such surface was 125–130 degrees, somewhat lower than on the APFC material coated with Teflon only (147 degrees). It may be explained by multiple dip coating operations that tend to reduce its "surface roughness" by folding the protruding fibers back into the surface.

5.3 Electrowetting tests

The electrowetting tests on the AFPC glass fiber material with the Bayton/parylene/Teflon coating have been performed in a typical configuration when a droplet of an electrolyte was placed on the surface of the filter material, with one contact made to the filter material and the other

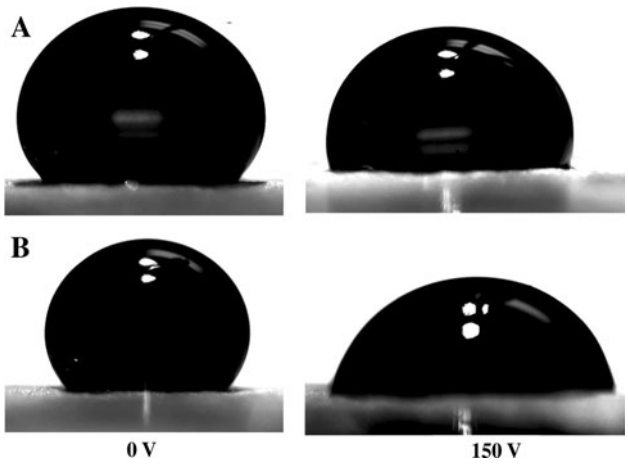

Fig. 7 Droplet shape before and after electrowetting transitions on APFC substrate. **a** propylene carbonate; **b** EC-DMC electrolyte

with the droplet via a platinum wire. In all tests, the filter material was at the ground potential. Given our main focus of using these materials in the construction of energy storage micro-batteries, we decided to use common electrolytes used in Li battery industry, as the test liquids for the electrowetting tests. We used propylene carbonate (surface tension 41.9 mN/m), a proprietary ethylene/dimethyl carbonate electrolyte (surface tension ~30–35 mN/m), as well as aqueous electrolyte based on $ZnCl_2/NH_4Cl$, used in our early studies [23, 24].

The tests were performed using a video capture arrangement of our contact angle measurement tool, VCA Optima, which allowed us to capture the images of the droplets before and after the electrowetting transition (EW), as well as to quickly measure the contact angle, Fig. 7. Clear electrowetting transitions have been observed for test liquids, with the activation voltage in 90–110 V range; photos on Fig. 7 show EW recorded at 150 V applied voltage.

Following a widely accepted capacitive model of electrowetting transitions [6, 42], the cosine of the measured contact angle should be proportional to a square of voltage. We plotted experimentally obtained data in Fig. 8. One can see a clear trend in the cosine before and after the electrowetting transition when plotted against V^2. A sharp transition from superhydrophobic to hydrophilic state occurs at around 90–110 V (8,100–12,100 V^2 on Fig. 8), depending on the liquid. In agreement with the earlier tests [6, 10], liquids with lower surface tension show lower contact angles before and after the EW transition. Contact angle saturation after EW transition is clearly seen, as is often the case in most of the EW tests reported in literature. The EW characterization is still ongoing. However, these early tests continue to indicate favorable results on the viability of this approach, to prepare "dielectric core/conductive polymer/dielectric/hydrophobic coating" structures using commercially available materials, bypassing the need

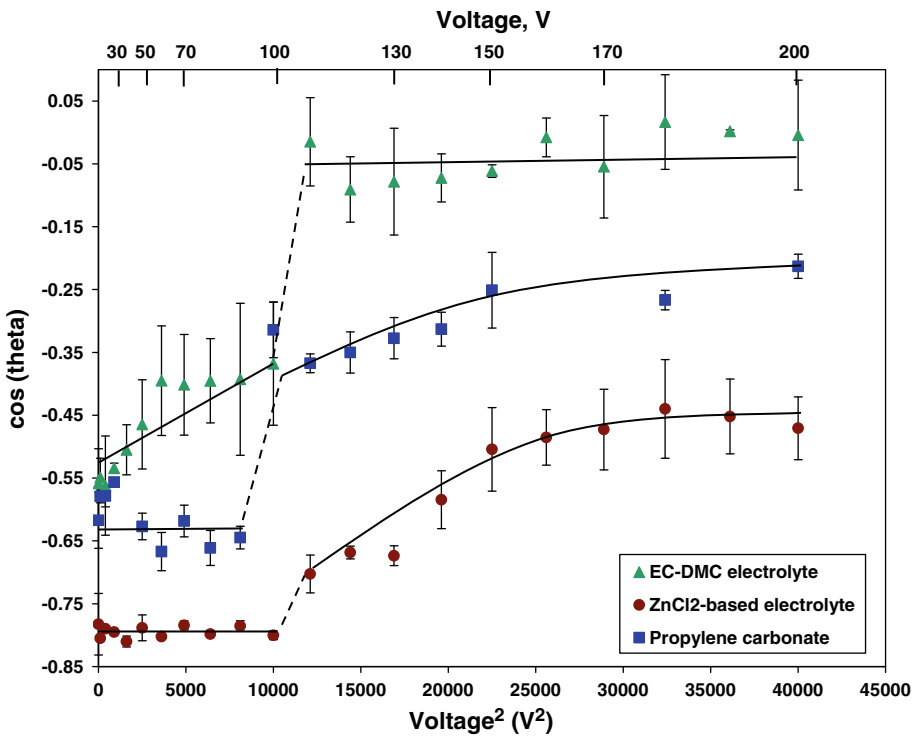

Fig. 8 Contact angle as a function of the applied voltage. Clear EW transitions are seen. *Solid lines* are given as a guide for the eye only

for clean-room environment and specialized microelectronic fabrication tools.

6 Conclusions

In summary, in this article we have presented a simple and effective route to prepare superhydrophobic materials using readily available glass fiber filters. The bends and kinks in the fibers give rise to the "roughness" on micro and nano-scale appropriate for obtaining superhydrophobic properties. The hydrophobic coatings were prepared from a variety of sources, such as vapor and solution deposited self-assembled alkyl-silane monolayers, dip coatings of fluoropolymers such as Teflon and CYTOP. A bi-layer material having one side highly hydrophilic and the opposite side superhydrophobic was prepared, by briefly exposing only one side of superhydrophobic fiber material to O_2 plasma, to remove the hydrophobic layer. The opposite side of the bi-layer material, protected from plasma side remains superhydrophobic. The material can absorb and wick liquids similar to the regular filter material and at the same time repel a wide variety of organic and aqueous liquids. Tunable electrowetting transitions have been demonstrated on the glass fiber materials impregnated with PEDOT–PSS conductive polymer and coated with parylene as a dielectric and Teflon as a hydrophobic coating. Applicability of these structures to creating microfluidic devices and separators for reserve micro-batteries has been discussed.

Acknowledgments Continued support by mPhase Technologies is greatly appreciated.

References

1. P.-G. de Gennes, F. Brochard-Wyart, D. Quere, *Capillarity and Wetting Phenomena: Drops, Bubbles, Pearls, Waves*. (Springer, New York, 2003)
2. D. Quere, Rep. Prog. Phys. **68**, 2495–2532 (2005)
3. D. Quere, Ann. Rev. Mat. Sci **38**, 71–99 (2008)
4. L. Gao, T. McCarthy, Langmuir **22**, 5998–6000 (2006)
5. L. Gao, T. McCarthy, Langmuir **25**, 14105–14115 (2009)
6. T.N. Krupenkine, J.A. Taylor, T.M. Schneider, S. Yang, Langmuir **20**, 3824–3827 (2004)
7. L.B. Boinovich, E.M. Emelyanenko, Rus. Chem. Rev. **77**, 583–600 (2008)
8. M. Nosonovsky, B. Bhushan, Microsys. Tech. **12**, 273–281 (2006)
9. M. Nosonovsky, B. Bhushan, Microsys. Tech. **11**, 535–549 (2005)
10. A. Ahuja, J.A. Taylor, V. Lifton, A.A. Sidorenko, T.R. Salamon, E.J. Lobaton, P. Kolodner, T.N. Krupenkin, Langmuir **24**, 9–14 (2008)
11. A. Tuteja, W. Choi, M. Ma, J.M. Mabry, S.A. Mazzella, G.C. Rutledge, G.H. McKinley, R.E. Cohen, Science **318**, 1618–1622 (2007)
12. A. Tuteja, W. Choi, J.M. Mabry, G.H. McKinley, R.E. Cohen, PNAS **105**, 18200–18205 (2008)
13. C. Neinhuis, W. Barthlott, Ann. Biol. **79**, 667–677 (1997)
14. V.A. Lifton, S. Simon, In: *Bionanotechnology: Global Prospects*, ed. by D.E. Reisner (CRC Press: Boca Raton, FL, 2008), p. 177
15. W. Barthlott, C. Neinhuis, Planta **202**, 1–8 (1997)
16. Y.T. Cheng, D.E. Rodak, C.A. Wong, C.A. Hayden, Nanotechnology **17**, 1359–1362 (2006)
17. A.R. Parker, C.R. Lawrence, Nature **414**, 33 (2001)
18. H.F. Bohm, W. Federle, PNAS **101**, 14138–14143 (2004)
19. V.A. Lifton, J.A. Taylor, B. Vyas, P. Kolodner, R. Cirelli, N. Basavanhally, A. Papazian, R. Frahm, S. Simon, T. Krupenkin, Appl. Phys. Lett. 93, 043112–043113-3 (2008)
20. A. Nakajima, K. Hashimoto, T. Watanabe, K. Takai, G. Yamauchi, A. Fujishima, Langmuir **16**, 7044–7047 (2000)
21. J. Zimmermann, G.R.J. Artus, S. Seeger, J. Adh. Sci. Tech. **22**, 251–263 (2008)
22. F.C. Cebeci, Z. Wu, L. Zhai, R.E. Cohen, M.F. Rubner, Langmuir **22**, 2856–2862 (2006)
23. V.A. Lifton, S. Simon, R.E. Frahm, Bell Labs Tech. J. **10**, 81–85 (2005)
24. V.A. Lifton, S. Simon, F.M. Allen, in *Proceedings of NSTI* (Boston, 2008)
25. H.F. Hoefnagels, D. Wu, G. de With, W. Ming, Langmuir **23**, 13158–13163 (2007)
26. nGimat Co., http://www.ngimat.com/pdfs/Nanoengineered_Surfaces_Self_Cleaning.pdf Integrated Surface Technologies http://www.insurftech.com/
27. H.M. Shang, Y. Wang, K. Takahashi, G.Z. Cao, D. Li, Y.N.J. Xia, Mater. Sci. **40**, 3587–3591 (2005)
28. M. Ma, Y. Mao, M. Gupta, K.K. Gleason, G.C. Rutledge, Macromolecules **38**, 9742–9748 (2005)
29. D. Han, A.J. Steckl, Langmuir **25**, 9454–9462 (2009)
30. Unless indicated otherwise, all contact angle data discussed in the manuscript are for the advancing contact angle
31. J. Zimmermann, M. Rabe, G.R.J. Artus, S. Seeger, Soft Matter **4**, 450–452 (2008)
32. A.W. Martinez, S.T. Phillips, G.M. Whitesides, PNAS **105**, 19606–19611 (2008)
33. D.A. Brevnov, M.J. Barela, M.J. Brooks, G.P. Lopez, P.B. Atanassov, J. Electrochem. Soc. **151**, B484–B489 (2004)
34. S.M. Mukhopadhyay, P. Joshi, S. Datta, G. Zhao, P. France, J. Phys. D Appl. Phys. **35**, 1927–1933 (2002)
35. B. Balu, V. Breedveld, D.W. Hess, Langmuir **24**, 4785–4790 (2008)
36. B. Balu, J.S. Kim, V. Breeveld, D.W. Hess, J. Adh. Sci. Tech **23**, 361–380 (2009)
37. B. Balu, A.D. Berry, D.W. Hess, V. Breedveld, Lab Chip **9**, 3066–3075 (2009)
38. www.hcstark.com
39. K. Bhat, J. Heikenfeld, M. Agarwal, Y. Lvov, K. Varahramyan, Appl. Phys. Lett. **91**, 024103–024103-3 (2007)
40. M. Agarwal, Y. Lvov, K. Varahramyan, Nanotechnology. **17**, 5319–5319 (2006)
41. L. Hu, J.W. Choi, Y. Yang, S. Jeong, F. La Mantia, L.F. Cui, Y. Cui, PNAS. **106**, 21490–21494 (2009)
42. F. Mugele, J.-C. Baret, J. Phys. Condens. Matter. **17**, R705–R774 (2005)